

SCIENTIFIC REPORTS



OPEN

Mechanically durable liquid-impregnated honeycomb surfaces

Philip S. Brown & Bharat Bhushan 

Liquid repellent surfaces typically work by keeping the fouling liquid in a metastable state, with trapped pockets of air between the substrate and the liquid. An alternative method with greater long-term stability utilizes liquid-impregnated surfaces, where the liquid being repelled slides over an immiscible liquid immobilized on a porous surface. Here, we report a method for creating honeycomb surfaces amenable to liquid-impregnation. Polystyrene dissolved in a water-immiscible, volatile solvent was deposited in a humid environment on a variety of substrates to achieve the necessary porosity. Evaporative cooling results in condensation of water in a breath figure array of droplets, forming a sacrificial template for the drying polymer film. These honeycomb surfaces were further functionalized with fluorosilane and dipped in the lubricating liquid to result in a durable, liquid-repellent surface. These surfaces were found to exhibit repellency towards water and oils with extremely low tilt angles due to the smooth liquid–liquid contact between the lubricating liquid and the liquid being repelled.

A range of desirable surface properties such as anti-fouling, self-cleaning, and anti-smudge repellency all rely on altering both the chemistry and roughness of a surface to achieve liquid repellency^{1,2}. Extreme water repellency, also known as superhydrophobicity, is where the contact angle of water on a surface is greater than 150° and the contact angle hysteresis (difference between advancing and receding contact angles) is less than 2°. This allows the liquid droplet to roll off the surface with no contamination. This repellency is typically achieved by roughening a hydrophobic surface, increasing the solid surface area in contact with the droplet³. Alternatively, air can become trapped between the surface and the liquid⁴.

Liquid repellency becomes more difficult when the surface tension of the liquid to be repelled is low. This is true for oils, since oil droplets typically exhibit contact angles of <90° on flat surfaces (oleophilic). However, high repellency via the Cassie-Baxter state of wetting can still be achieved through the use of re-entrant surface features, where the asperities create an overhang (i.e. become narrower closer to the surface)^{5–9}. However, such a configuration whereby air is trapped between the droplet and surface is only metastable state and, via applied pressure or surface vibration, the liquid will eventually penetrate into the roughness and fully wet the surface.

An alternate method of creating liquid-repellent surfaces is to take inspiration from the *Nepenthes* pitcher plants, which features a microstructured surface that is wet by nectar and rainwater to result in a continuous liquid film¹⁰. When wet, this region becomes extremely slippery and insects aquaplane across the surface and fall into the pitcher. There are several examples of pitcher plant-inspired, liquid-impregnated surfaces. These previous examples have several drawbacks that potentially limit their applicability to a range of scenarios. Teflon nanofibres and epoxy-molded nanoposts have previously been utilized as the required porous solid surface¹¹. However, such examples are unsuitable for certain real world applications due to their composition, fragility, and cost of fabrication.

Other previous examples rely on specific substrates. One such embodiment requires an oxide substrate for colloidal templating of a highly ordered porous monolayer¹². Other liquid-impregnated repellent surfaces have been reported on nano-textured alumina¹³ and electrodeposited polypyrrole nanostructures¹⁴. One substrate-independent method potentially more suited to a range of applications utilizes a spray coated porous wax layer¹⁵. However, the durability of a porous wax coating remains unclear. More recently, a mechanically durable liquid-repellent polypropylene coating was achieved through the creation of a liquid-impregnated porous polymer surface. Porous polypropylene was created through the use of a solvent–nonsolvent polymer solution¹⁶.

One alternative approach for the fabrication of porous surfaces is to utilise breath figures^{17,18}. Breath figures are two-dimensional hexagonally packed arrays of water droplets condensed onto a cooled surface. Such a breath figure can form on a drying polymer film surface, so long as the solvent used to cast the film is immiscible with

Nanoprobe Laboratory for Bio- & Nanotechnology and Biomimetics (NLBB), The Ohio State University, 201W. 19th Avenue, Columbus, OH, 43210-1142, USA. Correspondence and requests for materials should be addressed to B.B. (email: Bhushan.2@osu.edu)

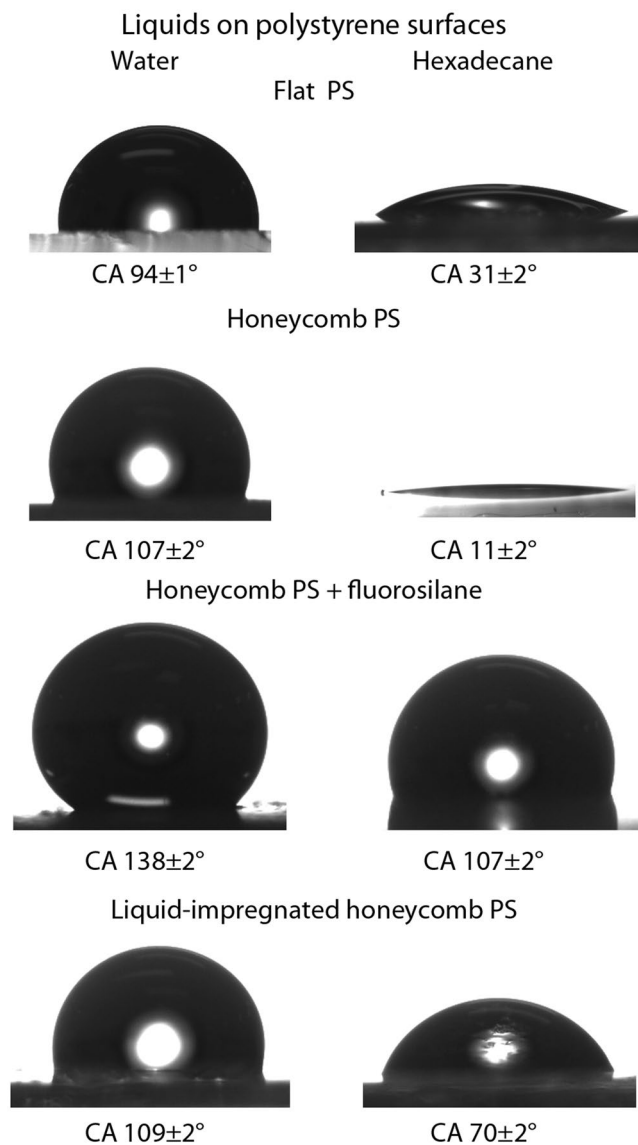


Figure 2. Contact angle images for droplets water and hexadecane on polystyrene surfaces.

perfluoropolyether (Krytox GPL 102, Dupont) with a chemical structure of $F-(CF(CF_3)-CF_2-O)_n-CF_2CF_3$, where $n = 10-60$, a surface tension of $16-20 \text{ mN m}^{-1}$, and a viscosity of 38 cSt.

Contact angle and tilt angle. For contact angle data, droplets of both water ($5 \mu\text{L}$, surface tension 72 mN m^{-1}) and n-hexadecane ($5 \mu\text{L}$, 99%, Alfa Aesar, surface tension 27 mN m^{-1} (ref. 24)) were dispensed onto the surface of samples using a goniometer (Model 290, Ramé-Hart Inc.) with the resulting droplet shape analyzed with DROPimage software. Tilt angles were determined by moving the surface until the $5\text{-}\mu\text{L}$ droplet was observed to slide off. All angles reported are the average of five separate measurements performed on different areas of a sample.

Optical imaging. Optical images were taken with a CCD camera (Nikon Optihot-2) to determine the topography of the polystyrene samples.

Wear experiments. The mechanical durability of the surfaces was examined through macrowear experiments performed with an established procedure of using a ball-on-flat tribometer, initially described elsewhere^{2, 8, 25}. Briefly, a 3-mm sapphire ball with an applied load of 10 mN normal to the surface was put into reciprocating motion for 200 cycles (stroke length = 6 mm, average linear speed = 1 mm s^{-1}). Optical images were taken before and after the experiment to track the formation of a wear scar.

Contact pressures were calculated based on Hertz analysis²⁵. For the surface, an elastic modulus of 3 GPa and a Poisson's ratio of 0.35 were used²⁶. For the sapphire ball, an elastic modulus of 390 GPa and Poisson's ratio of 0.23. The mean contact pressure was calculated as 14 MPa.

Optical image of honeycomb PS surface

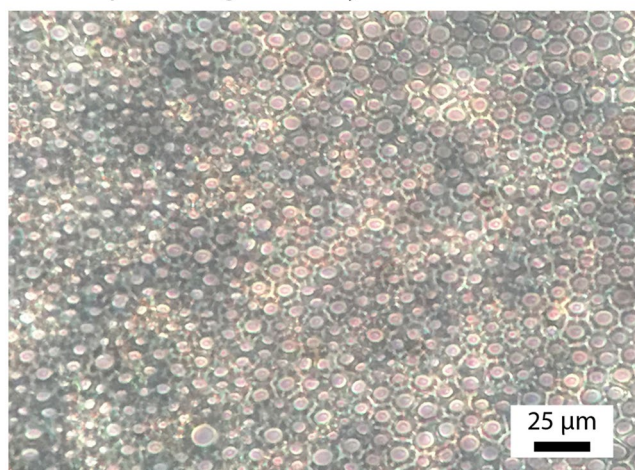


Figure 3. Optical images of a honeycomb surface on glass after solvent casting polystyrene from a water-immiscible, volatile solvent in a humid environment.

Wear experiment using ball-on-flat tribometer

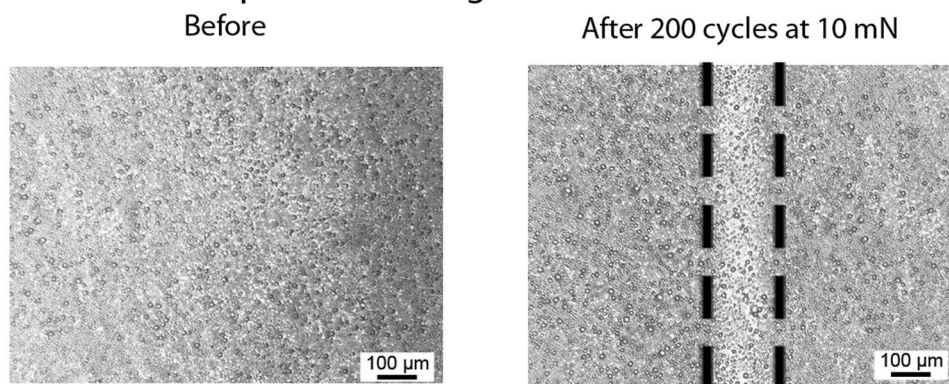


Figure 4. Optical micrographs before and after wear experiments using ball-on-flat tribometer using a 3-mm diameter sapphire ball at 10 mN loading on a honeycomb surface.

Results and Discussion

Flat polystyrene (PS) is found to be slightly hydrophobic with water contact angles of $94 \pm 1^\circ$, Table 1 and Fig. 2. In order to create the porous polymer surface, polystyrene was dissolved in a water immiscible, volatile solvent. A drop of the solution was cast onto a substrate and dried in a humid environment at room temperature. Evaporative cooling of the drying polymer film results in the condensation of water droplets and the formation of a breath figure. This array of water droplets acts as a sacrificial template for the drying polymer film and, once evaporation of the solvent and water is complete, results in a porous, honeycomb surface structure, Fig. 3. Fully dried, the polystyrene honeycomb surface was found to have a water contact angle of $107 \pm 2^\circ$ due to the increase in surface roughness.

The mechanical durability of the polystyrene honeycomb surface was investigated through the use of tribometer wear experiments and the resulting optical images, showing a portion of the wear track, are displayed in Fig. 4. The wear experiments were carried out with a load of 10 mN, with the tribometer put in reciprocating motion for 200 cycles. The images confirm that the polymer coating is not removed from the glass substrate. The density of the honeycomb structure appears to decrease in the wear location due to plastic deformation of the polymer. However, the porous structure is not completely destroyed, allowing for the impregnating liquid to remain in the wear region. It is believed that these surfaces can likely be more durable than many other examples of liquid-impregnated surfaces, which typically rely on poorly adhered wax coatings¹⁵ or delicate surface structures¹¹.

For the lubricating liquid to fully penetrate the porous surface, the chemistry of the honeycombs was altered, ensuring favorable wetting and no preferential dewetting when another liquid is added on top of the lubricating liquid layer. The polystyrene honeycomb coating was activated via UV irradiation to activate the surface for silane attachment. Following fluorosilane treatment, the polystyrene honeycomb surface displayed water contact angles

Oil droplets on tilted polystyrene surfaces

Untreated PS



Liquid-impregnated honeycomb PS

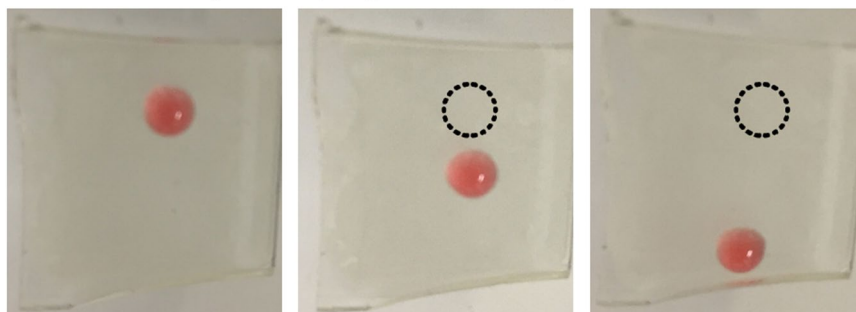


Figure 5. Photographs demonstrating hexadecane repellency of liquid-impregnated honeycomb surface compared to a fluorinated honeycomb sample.

of $138 \pm 2^\circ$ and hexadecane contact angles of $107 \pm 2^\circ$, Fig. 2. This altering of the surface energy is necessary to ensure that the lubricating liquid, in this case a lower surface tension fluorinated oil, will remain impregnated in the honeycomb structure and will not be preferentially replaced by the liquid to be repelled.

Finally, the honeycomb surface was dipped into the lubricating liquid. Following this, the liquid-impregnated surface exhibited water contact angles of $109 \pm 2^\circ$ and hexadecane contact angles of $70 \pm 2^\circ$, Fig. 2. However, due to the presence of the lubricating liquid, the surface displays very low tilt angles of $2 \pm 1^\circ$ and $4 \pm 2^\circ$ for water and hexadecane respectively, Table 1. Because the low tilt angles are a product of the homogeneity of the liquid–liquid interface, the surface tension of the liquid being repelled has little effect on the repellency of the surface.

The low tilt angle means that liquid droplets placed on the surface are able to slide over the surface easily. In Fig. 5, droplets of hexadecane were added to fluorosilane-treated honeycomb and liquid-impregnated honeycomb surfaces. Hexadecane droplets on the fluorosilane-treated surface are not easily removed when the surface is tilted due to high hysteresis and droplet pinning. In contrast, as the liquid-impregnated surface is tilted, the hexadecane droplet slides across the surface with very little resistance. The red dye present in the hexadecane droplet helps to confirm that the vacated area of the surface is not contaminated by the hexadecane. Further wear experiments carried out on honeycomb surfaces containing the lubricating liquid did not result in any change in the repellent properties of the surface, with droplets of hexadecane sliding over the wear location with no noticeable degradation in the repellency.

In certain applications, liquid-impregnated surfaces can exhibit greater long-term repellency than traditional liquid-repellent surfaces, the repellency of which is dependent on metastable states and trapped air. For instance, liquid-impregnated surface treatments could be better suited for applications where the contaminant liquid is in constant contact with the surface for extended periods of time or where the substrate is subject to vibration.

Conclusions

Liquid-repellent, slippery surfaces have been created on glass and polymer substrates via the formation of a honeycomb structure. Following UV activation and fluorosilane coupling to reduce the surface energy of the honeycombs, the substrate was dipped in a lubricating liquid, which became impregnated within the pores. This lubricating liquid layers repels other liquids placed on the surface through immiscible liquid–liquid contact. This results in very low tilt angles with droplets of both water and hexadecane sliding across the surface with no contamination. Such liquid-repellent surfaces will be more stable than repellent surfaces relying on the Cassie-Baxter state of wetting, where the liquid droplet being repelled is in a metastable state.

References

1. Bhushan, B. *Biomimetics: Bioinspired Hierarchical-Structured Surfaces for Green Science and Technology*, 2nd ed. (Springer International, Switzerland, 2016).
2. Brown, P. S. & Bhushan, B. Mechanically durable, superoleophobic coatings prepared by layer-by-layer technique for anti-smudge and oil-water separation. *Sci. Rep.* **5**, 8701 pp 1–9 (2015).
3. Wenzel, R. N. Resistance of Solid Surfaces to Wetting by Water. *Ind. Eng. Chem.* **28**, 988–994 (1936).
4. Cassie, A. B. D. & Baxter, S. Wettability of porous surfaces. *Trans. Faraday Soc.* **40**, 546–551 (1944).
5. Nosonovsky, M. & Bhushan, B. *Multiscale Dissipative Mechanisms and Hierarchical Surfaces* (Springer-Verlag, Heidelberg, Germany, 2008).
6. Tuteja, A., Choi, W., Mabry, J. M., McKinley, G. H. & Cohen, R. E. Robust omniphobic surfaces. *Proc. Natl. Acad. Sci.* **105**, 18200–18205 (2008).
7. Brown, P. S. & Bhushan, B. Designing bioinspired superoleophobic surfaces. *APL Mater.* **4**, 015703 (2016).
8. Brown, P. S. & Bhushan, B. Durable, superoleophobic polymer–nanoparticle composite surfaces with re-entrant geometry via solvent-induced phase transformation. *Sci. Rep.* **6**, 21048 pp 1–11 (2016).
9. Brown, P. S. & Bhushan, B. Durable superoleophobic polypropylene surfaces. *Phil. Trans R. Soc. A* **374**, 20160193 pp 1–9 (2016).
10. Bohn, H. F. & Federle, W. Insect aquaplaning: *Nepenthes* pitcher plants capture prey with the peristome, a fully wettable water-lubricated anisotropic surface. *Proc. Natl. Acad. Sci.* **101**, 14138–14143 (2004).
11. Wong, T.-S. *et al.* Bioinspired self-repairing slippery surface with pressure-stable omniphobicity. *Nature* **477**, 443–447 (2011).
12. Vogel, N., Belisle, R. A., Hatton, B., Wong, T.-S. & Aizenberg, J. Transparency and damage tolerance of patternable omniphobic lubricated surfaces based on inverse colloidal monolayers. *Nature Commun.* **4**, 2176 pp 1–10 (2013).
13. Ma, W., Higaki, Y., Otsuka, H. & Takahara, A. Perfluoropolyether-infused nano-texture: a versatile approach to omniphobic coatings with low hysteresis and high transparency. *Chem. Commun.* **49**, 597–599 (2013).
14. Kim, P. *et al.* Liquid-Infused Nanostructured Surfaces with Extreme Anti-Ice and Anti-Frost Performance. *ACS Nano* **6**, 6569–6577 (2012).
15. Smith, J. D. *et al.* Self-lubricating surfaces for food packaging and food processing equipment. US8 535, 779B1 (2013).
16. Brown, P. S. & Bhushan, B. Liquid-impregnated porous polypropylene surfaces for liquid repellency. *J. Colloid Interf. Sci.* **487**, 437–443 (2017).
17. Rayleigh, L. Breath Figures. *Nature* **86**, 416–417 (1911).
18. Widawski, G., Rawiso, M. & François, B. Self-organized honeycomb morphology of star-polymer polystyrene film. *Nature* **369**, 387–389 (1994).
19. Stenzel, M. H., Barner-Kowollik, C. & Davis, T. P. Formation of honeycomb-structured, porous films via breath figures with different polymer architectures. *J. Polym. Sci. Part A: Polym. Chem.* **44**, 2363–2375 (2006).
20. Srinivasarao, M., Collings, D., Philips, A. & Patel, S. Three-Dimensionally Ordered Array of Air Bubbles in a Polymer Film. *Science* **292**, 79–83 (2001).
21. Peng, J., Han, Y., Yang, Y. & Li, B. The influencing factors on the macroporous formation in polymer films by water droplet templating. *Polymer* **45**, 447–452 (2004).
22. Ferrari, E., Fabbri, P. & Pilati, F. Solvent and Substrate Contributions to the Formation of Breath Figure Patterns in Polystyrene Films. *Langmuir* **27**, 1874–1881 (2011).
23. Zhang, P., Chen, H., Zhang, L., Ran, T. & Zhang, D. Transparent self-cleaning lubricant-infused surfaces made with large-area breath figure patterns. *Appl. Surf. Sci.* **355**, 1083–1090 (2015).
24. Haynes, W. M. *Handbook of Chemistry and Physics*, 95th ed. (CRC Press, Boca Raton, F. L., 2014).
25. Bhushan, B. *Introduction to Tribology*, 2nd ed. (Wiley, New York, 2013).
26. *Polystyrene*, <http://www.goodfellow.com/E/Polystyrene.html>, accessed February 18, 2017.

Author Contributions

P.S.B. performed the experiments and analyzed the data. P.S.B. wrote the main text and P.S.B. and B.B. participated equally in planning, execution, and review of the manuscript.

Additional Information

Competing Interests: The authors declare that they have no competing interests.

Publisher's note: Springer Nature remains neutral with regard to jurisdictional claims in published maps and institutional affiliations.



Open Access This article is licensed under a Creative Commons Attribution 4.0 International License, which permits use, sharing, adaptation, distribution and reproduction in any medium or format, as long as you give appropriate credit to the original author(s) and the source, provide a link to the Creative Commons license, and indicate if changes were made. The images or other third party material in this article are included in the article's Creative Commons license, unless indicated otherwise in a credit line to the material. If material is not included in the article's Creative Commons license and your intended use is not permitted by statutory regulation or exceeds the permitted use, you will need to obtain permission directly from the copyright holder. To view a copy of this license, visit <http://creativecommons.org/licenses/by/4.0/>.

© The Author(s) 2017